remote sensing

MDPI

Article

Dynamic Slicing and Reconstruction Algorithm for Precise Canopy Volume Estimation in 3D Citrus Tree Point Clouds

Wenjie Li [1], Biyu Tang [1], Zhen Hou [1], Hongbo Wang [1], Zongyu Bing [1], Qiong Yang [2] and Yongqiang Zheng [1,*]

[1] National Digital Planting (Citrus) Innovation Sub-Center, National Engineering Research Center for Citrus Technology, Citrus Research Institute, Southwest University, Chongqing 400712, China; lwj17395844880@email.swu.edu.cn (W.L.); tangbiyu@email.swu.edu.cn (B.T.)
[2] Fushun County Bureau of Agriculture and Rural Development, Zigong 643299, China
* Correspondence: zhengyq@swu.edu.cn

Abstract: Crop phenotyping data collection is the basis for precision agriculture and smart decision-making applications. Accurately obtaining the canopy volume of citrus trees is crucial for yield prediction, precise fertilization and cultivation management. To this end, we developed a dynamic slicing and reconstruction (DR) algorithm based on 3D point clouds. The algorithm dynamically slices nearby slices based on their proportional area change and density difference; for each slice point cloud, the average distance of each point from others is taken as the initial α value for the AS algorithm. This value is iteratively summed until it reconstructs the complete shape, allowing the volume of each slice shape to be determined. Compared with six point cloud-based reconstruction algorithms, the DR approach achieved the best results in removing perforations and lacunae (0.84) and exhibited volumetric consistency (1.53) that closely aligned with the growth pattern of citrus trees. The DR algorithm effectively addresses the challenges of adapting the thickness and number of canopy point cloud slices to the shape and size of the canopy in the ASBS and CHBS algorithms, as well as overcoming inaccuracies and incompleteness in reconstructed canopy models caused by limitations in capturing detailed features using the PCH algorithm. It offers improved adaptive ability, finer volume computations, better noise reduction, and anomaly removal.

Keywords: citrus tree; LiDAR; canopy volume; point cloud reconstruction; dynamic slicing

check for updates

Citation: Li, W.; Tang, B.; Hou, Z.; Wang, H.; Bing, Z.; Yang, Q.; Zheng, Y. Dynamic Slicing and Reconstruction Algorithm for Precise Canopy Volume Estimation in 3D Citrus Tree Point Clouds. *Remote Sens.* **2024**, *16*, 2142. https://doi.org/10.3390/rs16122142

Academic Editors: Francesco Pirotti and Mitsunori Yoshimura

Received: 13 May 2024
Revised: 7 June 2024
Accepted: 10 June 2024
Published: 13 June 2024

Copyright: © 2024 by the authors. Licensee MDPI, Basel, Switzerland. This article is an open access article distributed under the terms and conditions of the Creative Commons Attribution (CC BY) license (https://creativecommons.org/licenses/by/4.0/).

1. Introduction

Citrus cultivation is crucial for the rural revitalization of southern China, with China leading globally in terms of both total output and planting area. However, challenges such as low intelligence and mechanization levels, and incomplete information construction persist [1,2]. The fruit tree canopy is responsible for absorbing light during respiration and photosynthesis, providing essential nutrients and energy for growth. Thus, monitoring the canopy is vital for estimating tree biomass, growth, yield, water consumption, health status, and long-term productivity [3–7]. Moreover, obtaining canopy information enables the quantification of pruning effects and the evaluation of tree characteristics. It is vital in citrus tree production, breeding, and management, as it is inextricably associated with orchard precision management projects such as irrigation and fertilization practices, moisture detection techniques, fruit crop breeding, and yield assessment methods [8]. At the same time, accurate canopy volume measurements can serve as a foundation for determining crop pesticide doses and making decisions [9,10], as well as providing technical assistance for pruning robots [11] and assisting managers in making sound agricultural production decisions [12–14]. Therefore, the rapid and accurate estimation of canopy features plays a crucial role in monitoring fruit tree growth dynamics and enhancing orchard management optimization [15].

Citrus trees are evergreen perennials, and their canopy characteristics are key to understanding growth, yield, physiological markers, and growth conditions [16]. The

common methods for measuring canopy volume include manual and non-contact automatic measurements. Manual methods involve measuring tree height and width with tools like tape and height rulers, approximating the crown to a geometric model, and calculating volume using the model's formula. Miranda-Fuentes et al. [17] found that using the ellipsoid method for olive tree volume prediction yielded the best results, with an R^2 of 0.84. Zheng et al. [18] used an uneven columnar shape for Hamlin sweet orange trees, indicating that manual volume measurements can serve as growth and yield indicators. Lee et al. [19] introduced a novel method involving horizontally slicing the crown, measuring circumference with a PVC pipe, and calculating slice volume, resulting in lower errors compared to traditional manual measurements (−1.99% and 5.96%). Li et al. [20] improved this method by using a formula for a circular platform, achieving relative errors ranging from −0.28% to 4.22%, and an average error of 1.78%, making it more accurate than previous models. While manual measurements are simple and convenient, they are prone to subjective errors and significant differences between the model and the canopy's true form.

Researchers have developed various non-contact automatic measurement methods for efficient and accurate canopy measurements. Dong et al. [21] reconstructed an orchard using photographs taken by a camera-carrying UAV and extracted the area of a single fruit tree in two plots, with root mean square error (RMSE) values of 0.72 m^2 and 0.48 m^2, respectively, indicating that the method overestimates the fruit tree's area. Jurado et al. [22] employed a camera to capture numerous overlapping photos to estimate plant height and volume. Based on the data, the approach calculated the volume with an average inaccuracy of 0.4 m^3, indicating an issue with erroneous results. Cameras for 3D reconstruction have the benefit of being low-cost and rich in texture. Cameras, on the other hand, have the disadvantage of being readily limited by light and climatic conditions, requiring a high level of equipment and technology, complex data processing, and the necessity for vast amounts of data capture. Dong et al. [23] collected canopy volume, trunk diameter, tree height, and fruit number in an orchard by putting an RGB-D depth camera on a pole to gather data from a horizontal or top-down view, and then 3D reconstructed an apple tree using photos on both sides. Subsequently, they utilized these data to reconstruct a three-dimensional model of an apple tree by employing images taken from multiple angles. Based on reconstruction results, the algorithm's yield prediction accuracy across the three datasets was 0.91–0.94, with some underestimation issues. Yin et al. [24] employed depth cameras to generate a three-dimensional reconstruction of a cherry tree and perform volume calculations. The R^2 between predicted and actual values was 0.932, and the MAPE was 0.116, indicating some technical support for pruning in cherry trees. Although depth cameras are more precise and accurate in 3D reconstruction and are more sensitive to changes in light than are standard cameras, they nevertheless have drawbacks, including low-quality depth images and a small measuring range. A system built using wireless networks and ultrasonic sensors was created by Yu et al. [25] to achieve three-dimensional reconstruction and volume extraction from fruit tree canopy. This experiment showed volumetric results consistent with manual measurements (R^2 = 0.8972, RMSE = 1.766 m^3), but lacked comparison with related algorithms. In the study by H Maghsoudi et al. [26], ultrasonic sensors at various heights were placed on a sprayer to detect canopy information in real time, and then a multilayer perceptual neural network technique was used to calculate canopy volume. This experimental test data's MSE was 0.012, and R^2 was 0.9596, which can effectively support the precise application of medication. Measuring data using ultrasonic measurement technology has the advantages of being noncontact, highly efficient, and highly accurate; however, in practice, measurement results are easily influenced by environmental noise and temperature changes, and the detection range is limited, necessitating the use of multiple devices and complex technology. Zhang et al. [27] used tilt photography to create a linear relationship between the crop volume model and manually determined biomass. The results on the validation set (R^2 = 0.752, RMSE = 139.1 gm^{-2}, RE = 15.3%) showed that its R^2 was too low and still a long way from practical application. Zhu et al. [28] used tilt photography to determine the canopy structural parameters of maize. The experiment

extracted maize plant height, leaf length (R^2 = 0.91), leaf area (R^2 = 0.76), slightly higher RMSE and ME, but leaf area extraction needed further improvement. Tilt photography has the advantages of wide range and quick speed, but its measurement accuracy is greatly influenced by lighting conditions, background interference, camera distortion, and other variables. Because of the complicated canopy structure of fruit trees, tilt photography cannot reconstruct the bottom of the canopy and is easily influenced by environmental changes during acquisition.

Light Detection and Ranging (LiDAR) effectively manages information to characterize tree canopies, generating point clouds with high accuracy and fast data acquisition [29]. The algorithms that are often used by researchers for point cloud-based canopy reconstruction can be categorized into the envelope approach, envelope slicing approach and imitation polyhedral approach. The envelope approach generates an envelope along the outer contour of the tree crown. Lee et al. [19] employed a convex hull approach to determine the volume of Hamlin sweet orange trees, obtaining more valuable information for predicting tree growth and productivity. Mahmud et al. [30] employed the alpha-shape algorithm to estimate the volume of a fruit tree, with the canopy volume calculated by this algorithm showing a significant correlation with the physically counted foliage. The envelope approach advantages include low algorithm complexity, a simple structure, and a fast running speed. The disadvantages are that the target volume is typically overestimated and the internal structure of the target is ignored. The envelope slicing method is an improvement on the envelope method that primarily optimizes the internal structure so that the reconstruction can better detect internal holes and gaps, making the reconstruction results more accurate. Xu et al. [31] employed a convex hull slicing approach to determine the predicted volume and surface area of the canopy, lowering the computational error of complicated canopy structures. Liu et al. [32] proposed a slice-based alpha shape algorithm for canopy reconstruction and volume calculation of pomelo trees. The imitation polyhedral approach consists primarily of dividing the canopy into several similar polyhedra (such as square, dome, and cone) and then calculating the volumes of these polyhedra to obtain the total volume, which is suitable for further analyzing the canopy structure and determining leaf area. Chakraborty et al. [33] employed a handheld 3D LiDAR scanning device to determine the volume of a grapevine canopy, and they found that the voxel-based algorithm more accurately accounts for changes in canopy structure than does the convex hull algorithm. In a study by Wang Jia et al. [34], the tree crown was split into many uneven platforms, and the crown volume was obtained, but viewing the cross section of each point cloud slice as circular or elliptical resulted in a large deviation in the calculation results. Yang et al. [31] improved this platform method to determine the volume of the canopy by calculating the area of the convex packet of each crown point cloud slice, and precision improvement and fast reconfiguration of the canopy structure was achieved. Sections 2 and 3 will provide a more detailed description and evaluation of these algorithms.

Most agricultural researchers still use manual measurements of the volume of citrus orchard, which not only is time-consuming and laborious but also has a large deviation from the true volume, which is not conducive to further analysis by researchers. We summarize six typical point cloud reconstruction algorithms (PRAs) for reconstructing a citrus circle with 160 orange trees and propose a set of preprocessing procedures for 3D reconstruction of a large-scale citrus orchard using a handheld laser scanner. These algorithms include Convex Hull (CH), Alpha-Shape (AS), Platform Convex Hull (PCH), Voxel-based (VB), Convex Hull by Slices (CHBS), and Alpha-Shape by Slices (ASBS). We then synthesize the principles, geometric properties, volume values, runtime, and linear relationships with each algorithm to analyze the reconstruction effectiveness and problems. The efficacy and issues of each algorithm's outputs are evaluated. The findings demonstrate that even with the best performance of these six algorithms (the ASBS algorithm) used to reconstruct an orange tree, the thickness and number of canopy point cloud slices are not always able to match the size and shape of the canopy itself. Accordingly, we developed a dynamic slicing and reconstruction canopy volume algorithm (DR), which, compared to existing

algorithms, dynamically slices nearby slices based on their proportional area change and density difference, better capturing and reflecting the actual growth characteristics of the tree canopy. Dynamically updating α values based on average point spacing provides a smoother and more natural reconstruction of the slice region, improving volume computation accuracy. Finally, we integrate the benefits of each of the algorithms to identify acceptable operating fields for them, providing an effective reference for the intelligent mechanization of orchards in the future. Section 2 describes the preprocessing process of segmenting a single fruit tree, as well as the principal method and implementation process of each algorithm. Section 3 describes the experimental process and results with a detailed analysis. Section 4 discusses the influence of the number of slices on the reconstruction effect, followed by the application scenarios for each algorithm, and Section 5 presents the conclusions of this paper, together with research challenges and future prospects.

2. Materials and Methods

2.1. Test Area

The experimental citrus variety used was late-maturing blood orange No. 8, a trifoliate orange rootstock with a tree age of 3 years. Blood orange No. 8 is a bud mutation discovered in the descendants of Italian Tarocco blood oranges and is a late-maturing type among blood oranges [35]. Its main cultivation areas are in Sichuan Province and Chongqing Municipality, China. The trees are vigorous, with tree forms including round-headed, main stem shapes, and open-hearted. The experimental orchard has a spacing between rows of 5.5 m, a tree standing of approximately 2.5 m, and a plant distance of 2 m. The base adopts the method of high ridges with deep furrows for soil bundling, with the height of the ridges ranging from 0.3 to 0.6 m. The blood orange tree has a natural round head structure, which is more compact and full, with a slightly open posture, and the middle-length branches easily droop. The crown is more rounded, the branches are evenly distributed, and the bottom of the crown is densely foliated; however, there are also many holes and gaps. The experiment was conducted in December 2023 in Jingba village, Jielong town, Fushun County. The local area (29°12.78′N, 105°5.97′E) features an average altitude of 310 m above sea level, a mean yearly precipitation of 1081.69 mm, and a typical yearly temperature of 19.82 °C. It is located in the southwest Sichuan Basin and has a shallow hill landscape, a subtropical humid monsoon climate, abundant rainfall, abundant light, a lengthy frost-free period and four distinct seasons. Four rows totaling 160 blood orange trees were selected as the subjects of this experiment. Figure 1 shows the experimental site.



(**a**) (**b**)

Figure 1. Photographs of the experimental area: (**a**) Satellite image of a blood orange orchard; (**b**) ground-level image of a blood orange orchard.

2.2. Acquisition Device and Acquisition Method

The handheld 3D LiDAR scanning device (GoSLAM RS100 (Beijing SkySmart Aviation Technology Co., Ltd., Beijing, China)) consists of a laser scanning head and a data processing unit (Figure 2). The laser scanning head is made up of a laser emitter, receiver, and scanning mirror that allows quick scanning of the target surface. The data processing unit consists of an inertial measurement unit (IMU) for measuring device acceleration and angular velocity and a microcomputer for data processing, map generation, localization, and navigation activities. This device scans a distance of 120 m and has a scanning rate of 650,000 points/s, a point accuracy of 1 cm, 32 lines of laser lines, a scanning range of 360° × 285°, and two lithium batteries, allowing the LiDAR system to work continuously for 4 h.

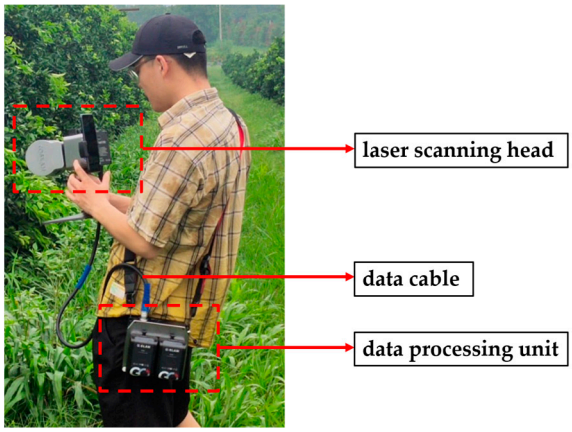


Figure 2. Constituent parts of the handheld 3D LiDAR scanning system (GoSLAM RS100).

The experimenter used a handheld LiDAR scanning device to collect scanning data in a closed loop around the experimental site line by line; the roadmap of the collection is shown in Figure 3. The laser scanner scans the experimental area along with the nearby environment during operation. The figure was produced after the experimental test area was delineated using the point cloud cropping and slicing function in the GoSLAM Studio (V2.0.53) point cloud processing software.

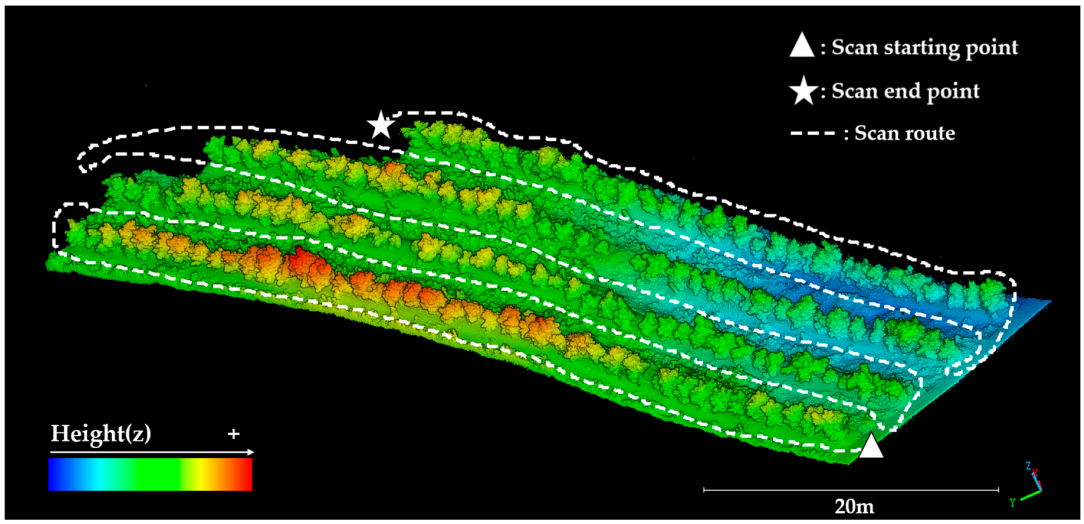


Figure 3. Three-dimensional LiDAR map of the blood orange orchard. The gradient color by z value indicates altitude; the white dashed line represents the path traveled by the LiDAR scanning equipment during the scan, and the triangle and star markers indicate the starting and ending points of the scan paths, respectively.

2.3. Preprocessing for Canopy Reconstruction

The canopy reconstruction preprocessing flow can be found in Figure 4. Initially, a 3D model of a blood orange orchard was created utilizing a LiDAR scanner. The experimental area was then cropped using GoSLAM Studio software. The CSF algorithm from the lidR package in RStudio was employed to filter ground points, followed by the application of the fast Euclidean clustering algorithm written in Python within PyCharm for segmenting individual fruit trees. Finally, the SOR algorithm in CloudCompare software (V2.13) was utilized to eliminate noisy points, and the unique() function, a built-in function in MATLAB R2023a, was used to remove repetitive points.

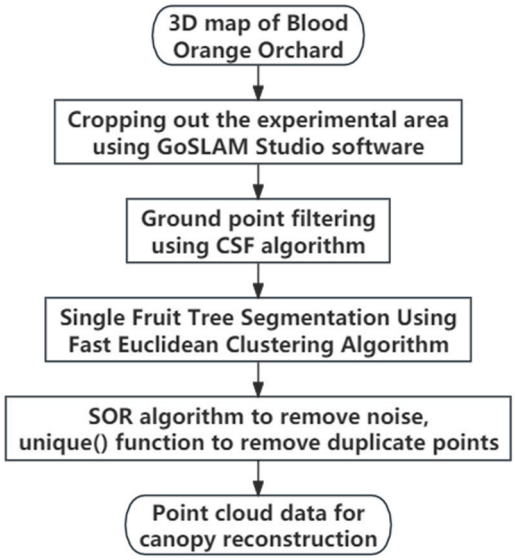


Figure 4. Preprocessing for canopy reconstruction flowchart. Note: CSF, cloth simulation framework algorithm; SOR, statistical outlier removal algorithm.

2.3.1. Ground Filtering

To facilitate the subsequent extraction of fruit tree information, it was necessary to select a suitable algorithm to filter the ground points in the test area. Common algorithms include least squares plane fitting (LSPF) [36], random sample consensus (RANSAC) [37], and the cloth simulation framework (CSF) [38]. The LSPF fits the ground plane model by minimizing the distance between the point and the plane. RANSAC is primarily used to fit the model and remove outliers, and it is commonly used to recognize simple geometric objects (such as planes and straight lines). Since the test area is a blood orange orchard with high ridges and deep furrows, the LSPF algorithm assumes that the ground is planar and cannot accurately identify ground points for orchard ground with irregular ground surfaces or large elevation variations. The RANSAC algorithm is also unable to accurately fit a complex ground model, is sensitive to noise and occlusions, and has high computational complexity and difficulty in parameter selection. The CSF algorithm can fully consider the local and global characteristics of point cloud data to better cope with complex orchard terrain. Through regional growth and point cloud segmentation technology, ground points can be accurately identified, a reliable ground model can be extracted, and a reliable database can be constructed. This paper thus employed the CSF algorithm.

The lidR package in RStudio includes the CSF function, which contains four parameters. sloop_smooth determines whether the point cloud is smoothed to decrease the impact of noise. The class_threshold function is used to modify the accuracy and stability of ground extraction by adjusting the threshold for dividing ground and nonground points. The cloth_resolution parameter is used to control the grid resolution of ground point cloud data to balance processing efficiency and ground extraction accuracy. The time_step parameter is used to control the rate at which the number of ground points increases. This study

employed four feature values: TRUE, 0.4, 1, and 1. Figure 5 shows the filtered results. Although certain dispersed weeds and ground points remained unfiltered, they had no effect on subsequent single-tree segmentation.

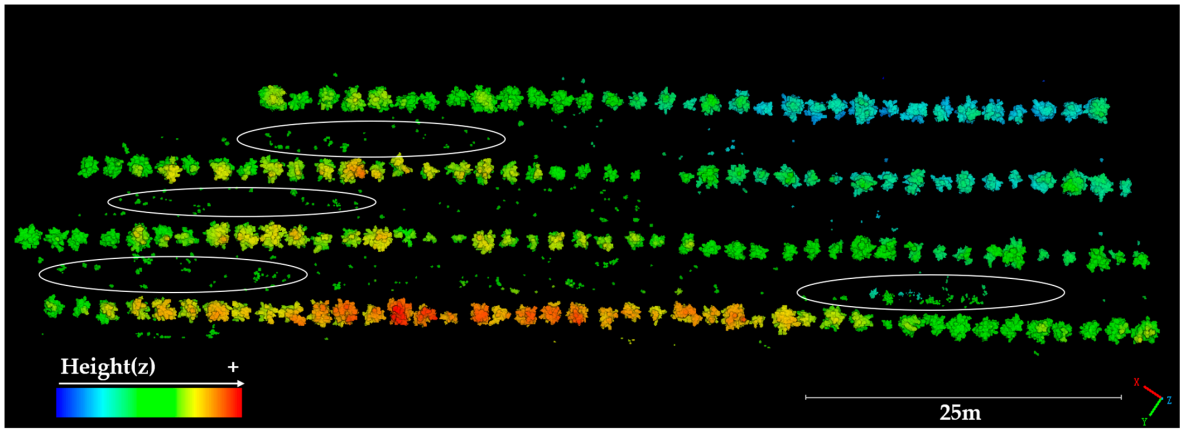


Figure 5. The experimental area after completing CSF ground filtering, with some weeds and ground points still present (indicated by white circles).

2.3.2. Single Fruit Tree Splitting

After finishing the ground filtering, the point cloud should be segmented by clustering using appropriate clustering algorithms in conjunction with the crop growth characteristics and the size of the test area to obtain each fruit tree's point cloud data. Among the frequently employed clustering algorithms are the region expanding algorithm [39] and the Kmean clustering [40], DBSCAN clustering [41] and Euclidean clustering [42] algorithms. The point cloud is split up by the region expanding algorithm into different regions based on the similarity between neighboring points to form point clusters with continuity. The Kmean clustering algorithm separates the point cloud data into a set of groups, with the centroid of each representing a grouping result. The DBSCAN clustering algorithm identifies and segments clusters based on the density of points. The Euclidean algorithm for clustering classifies point cloud data into discrete clusters based on their physical closeness, allowing for the identification and separation of unique objects or features within the dataset. Considering that there were 160 fruit trees in the test area, the point cloud file had close to 30 million points, and the file size was 1 GB. The computational complexity of the area growth algorithm was high. The Kmean clustering algorithm required a certain number of groups and numerous tests for fruit trees of various forms and densities and was highly reactive to noise. The DBSCAN algorithm was more sensitive to parameter selection, and the processing of large files was too time-consuming. Therefore, these algorithms were not suitable for processing large files of blood orange orchard point clouds. Liu et al. [32] chose to use Euclidean clustering for single tree segmentation of pomelo orchards containing 36 fruit trees and achieved good segmentation results, which shows that compared with traditional algorithms, Euclidean clustering algorithms are more suitable for citrus orchards. Yu et al. [43] proposed fast Euclidean clustering algorithms to optimize the data structure and algorithmic flow of the Euclidean clustering algorithm. The clustering data structure and algorithmic process avoids constantly traversing each point, and has higher efficiency and speed when dealing with large-scale point cloud data; therefore, this experiment adopted the fast Euclidean clustering algorithm for single tree segmentation.

The fast_euclidean_cluster() function was implemented in the open3d library in the Python environment, and the function contains four parameters. The tolerance parameter specifies the search range of the closest search. The parameter max_n represents the maximum number of points for a nearby search. The choice of this value affects the speed and accuracy of the clustering. The min_cluster_size parameter determines the

smallest number of points required for a group of points. The parameter max_cluster_size determines the largest number of points required for a group of points. Based on the real tree spacing, plant distance, and the number of points between the smallest and largest fruit trees within each row of the blood orange orchard, this paper set the values of the four parameters to 0.08, 800, 18,000, and 600,000, respectively. Figure 6 shows the clustering results after the algorithm had been run; each different color represents a fruit tree segmented out, and from the results, the fast Euclidean clustering method also removed scattered weeds and ground point clouds from the point cloud.

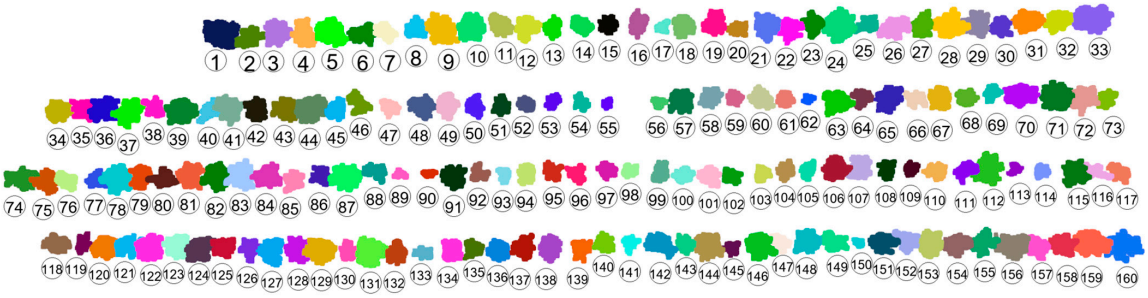
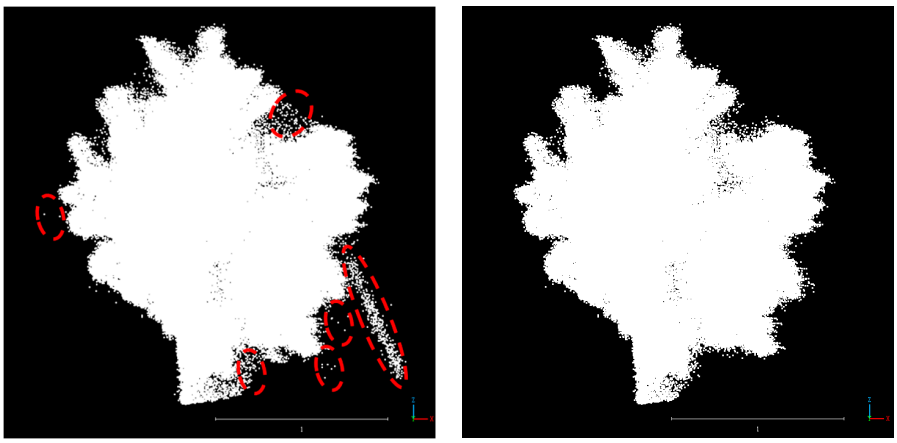


Figure 6. Clustering results for the blood orange orchard 3D map. Each different color represents a split fruit tree, manually numbered on the original image, indicating trees from 1 to 160.

2.3.3. Point Cloud Denoising and Deduplication

Laser scanning typically produces point cloud datasets of nonuniform density, and errors in measurements and environmental disturbances can also lead to the appearance of sparse outliers. Statistical Outlier Removal (SOR) algorithm [44] is used to remove obvious outliers, which indicates that a point cloud is considered invalid if it is less than a certain density. The SOR algorithm requires that the parameters k and n be set. The number of neighborhood points taken into account when determining the mean distance for each point is indicated by the expression "k number of nearest neighbors". The notation "n multiple of standard deviation" means that the algorithm, after determining the average distance between every single point, examines the distribution of distances for each point from a point cloud. If a point's distance exceeds the mean plus n multiplied by the norm deviation, that is thought to be an anomaly. In this study, it was experimentally found that when k = 600 and n = 3, not only were the noise points around the citrus tree point cloud effectively removed, but also, the original structure of the citrus tree point cloud was completely preserved. Figure 7 compares the data before and after denoising.



(**a**) (**b**)

Figure 7. Comparison of the data before and after denoising. (**a**) The data before denoising. The red dashed circle shows a few obvious noise points (including the stick used to support the branch). (**b**) The state after denoising.

Due to the movement of the scanner or the intricate structure inside the tree canopy, when scanning citrus trees with a laser scanner, the scanning region overlaps. This means that points at the same position are scanned more than once, resulting in duplicate points. Repetitive points can generate data bloat and impact the accuracy and efficiency of the reconstruction algorithm throughout further processing and analysis, particularly during AS reconstruction. Repetitive points make the algorithm process more data and cause the reconstruction results to have undesired concavities, convexities, or discontinuities. Point cloud duplicate points were removed using the unique (pointCloud, 'rows') function in MATLAB, which takes every single point from the point cloud as a row afterwards to locate the unique point within it. Duplicate points were removed for 160 test trees, with an average of 52 duplicate points removed per tree and an average time of 0.19 s per tree.

2.4. Calculating the Canopy Height and Width of Fruit Trees

Assessing the physical properties of fruit trees (e.g., tree height, crown spread, and canopy volume) is essential in agricultural studies and is increasingly a significant subject in precision agriculture [29]. Horticulturists can use accurate morphological estimates to evaluate the impact of these characteristics on crop output, wellness, and growth. Growers, when experimenting with various root stocks, determine which rootstock produces the most per unit volume in a given geographic region. They also utilize parameters such as the height of trees and crown spread when predicting fruit yield. This approach to assessment requires significant human effort and frequently lacks precision [23]. These geometric features for phenotyping are now available for extraction via LiDAR scanning. To assess the accuracy of the current scanner acquisition data, we manually measured the plant height and east-west and north-south crown widths of 160 blood orange fruit trees using a tape measure. For the LiDAR-scanned and preprocessed point clouds of individual fruit trees, we used CloudCompare software to calculate the minimum AABB box. The box's x and y lengths indicate the fruit tree's two canopy widths (W), and the z length indicates the fruit tree's height (H).

The H was determined uniformly with the following Formula (1):

$$H = Z_{\max} - Z_{\min} \tag{1}$$

where $Z_{\max}$ and $Z_{\min}$ represent the highest and lowest points of the Z elevation.

The W was calculated uniformly using the following Formula (2):

$$W = \frac{W_{NS} + W_{EW}}{2} \tag{2}$$

where W_{NS} represents the north–south width and W_{EW} represents the east–west width.

A comparative analysis of the canopy height (Table 1) and width (Table 2) measured by the two methods revealed a smaller error between H and W from laser scanning and manual measurement (RE of 0.039 for H and 0.081 for W), and the minimum RE values for H and W even reached 0.005 and 0.003, respectively. Therefore, the data processed using GOSLAM RS100 scanner offered greater precision in representing the real fruit tree morphology, which provided an accurate basis for later canopy volume calculations.

Table 1. Comparison of height values measured by manual and CC methods.

***H* (m)**	**Manual**	**CC**	**Absolute Error**	**Relative Error**
Mean	1.835	1.814	0.072	0.039
Var.	0.118	0.130	0.004	0.001
Max	2.590	2.616	0.397	0.178
Min	0.880	0.83	0.001	0.0005

Table 2. Comparison of the width values measured by the manual and CC methods.

W (m)	Manual	CC	Absolute Error	Relative Error
Mean	1.619	1.719	0.131	0.081
Var.	0.087	0.114	0.011	0.004
Max	2.400	2.460	0.513	0.343
Min	0.730	0.793	0.0005	0.0003

2.5. Canopy Reconstruction and Volume Calculations

The fruit canopies of the trees were reconstructed using manual measurement (MM) and 7 types of PRAs to compute canopy volume. These PRA algorithms were run using MATLAB R2023a.

2.5.1. MM Approach

Ellipsoidal models are frequently utilized by researchers as geometric models for typical citrus tree canopies [45]; hence, in this study, the ellipsoidal formulation was employed as the MM approach to determine the canopy volume of blood orange trees. The volume was computed with the following Equation (3):

$$V = \frac{\pi \cdot W^2 \cdot H}{6} \tag{3}$$

where W is crown width and H is the plant height, both of which were measured by the CloudCompare software above.

Figure 8a shows an image obtained with the manual method.

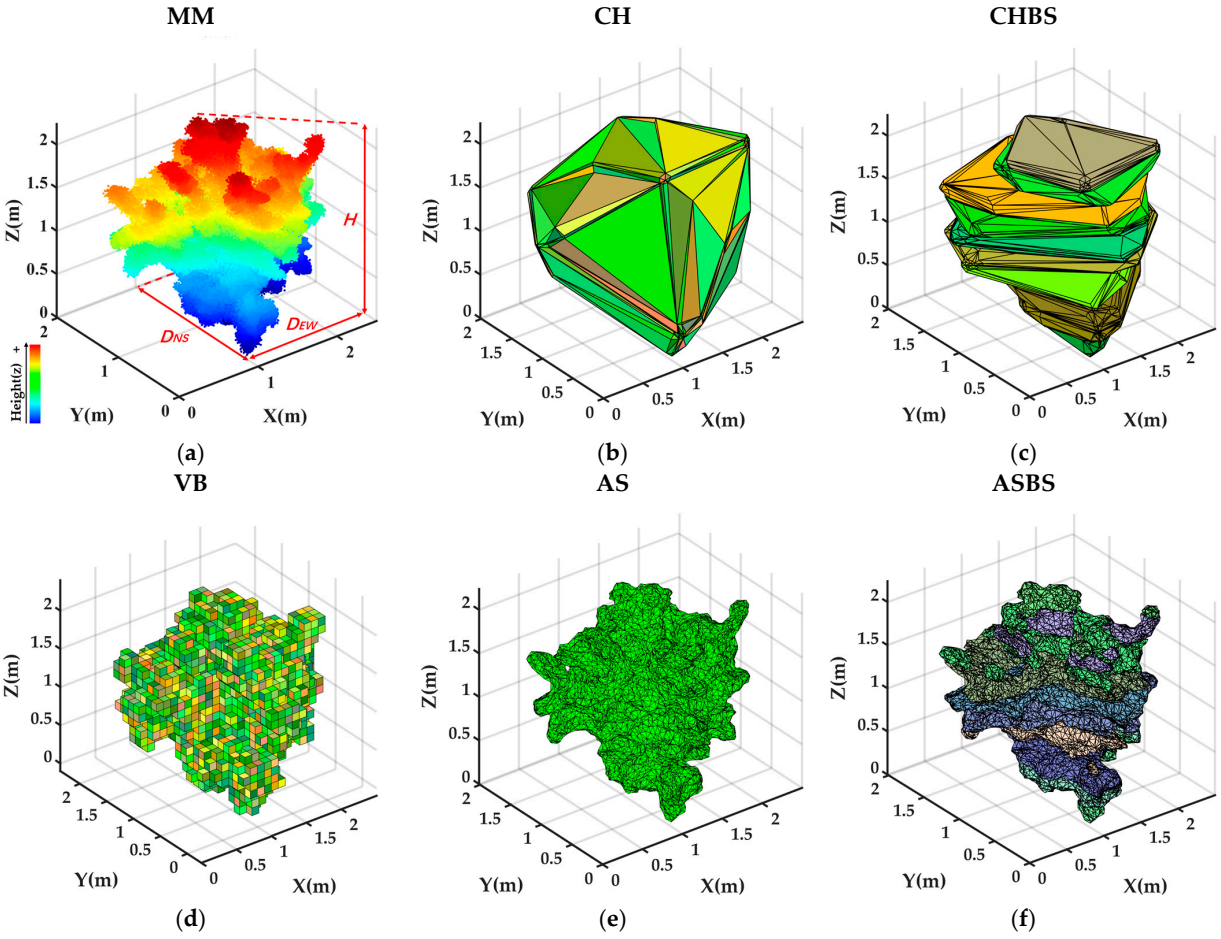


Figure 8. *Cont.*

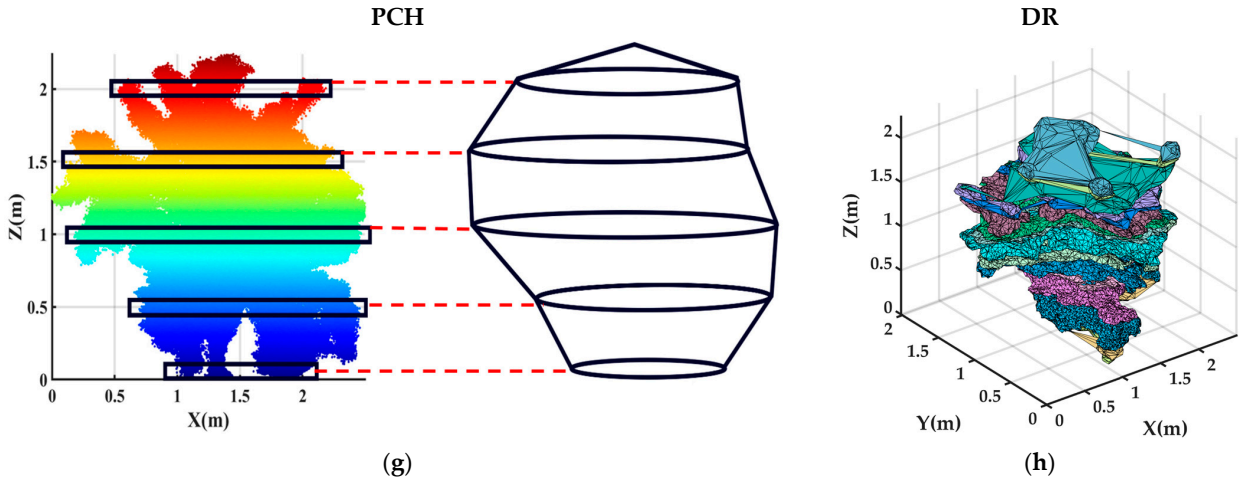


Figure 8. Canopy reconstruction effect diagram with (**a**) manual method (MM); (**b**) convex hull (CH); (**c**) convex hull by slices (CHBS); (**d**) voxel-based (VB); (**e**) alpha-shape (AS); (**f**) alpha-shape by slices (ASBS); (**g**) platform convex hull (PCH); (**h**) dynamic slicing and reconstruction (DR) algorithms. Note: x, y, and z denote the east–west width, north–south width, and height, respectively.

2.5.2. CH Approach

In computer graphics, a convex packet is the smallest convex set containing a finite set P of points in an arbitrary dimensional space. It consists of convex hull vertices and behaves like a convex solid in a three-dimensional environment. In this study, the QuickHull method was used to determine the volume of a convex hull on the surface of a citrus tree. Figure 8b depicts the canopy reconstruction effect diagram using a CH algorithm.

2.5.3. CHBS Approach

The CHBS approach works by taking a specific number N of equally spaced slices of the point cloud in the z-direction after running the CH algorithm on each segmented point cloud slice to determine the slice volume. Finally, the total volume within the canopy is computed by adding the volumes of the individual slices. Various numbers of slices had varying effects on the experimental results, and Yan initially selected a 15 cm spacing in his slice investigation since estimating the volume using the CH or AS algorithms required at least three points per slice [46]. In this study, the mean value of H was 1.835 m (Table 1); hence, the value of N was set at 10. Figure 8c depicts the canopy reconstruction effect diagram using the CHBS algorithm.

2.5.4. VB Approach

The VB approach works on the premise of segmenting the tree crown in the tree height direction in k steps of equal distance. The points in each segment of the canopy are projected onto a plane perpendicular to the tree height direction, and then the plane is divided into image elements of size k × k. Determined by the number of dots projected into every graphic element, the validity of the image element is judged, and the number T of valid image elements is counted. Finally, the volume of the canopy can be expressed as the sum of the T k × k × k voxel elements. Lecigne [47] proposed that when k equals one-tenth of the width of the canopy, the calculations are stable. In this investigation, the mean value of W was 1.619 m (Table 2); hence, the value of k was set to 0.1 m. Figure 8d depicts the canopy reconstruction effect diagram using the VB algorithm.

2.5.5. PCH Approach

The PCH algorithm views the entire canopy of a fruit tree from bottom to top as a geometry composed of many platforms and a cone [48]. First, the canopy's point cloud data are sliced based on elevation. Subsequently, every slice is inserted into a convex packet of planar point sets using the Graham convex packet algorithm. The area of the convex packet

(S) is then determined using Green's formula; thus, the volume of each platform is obtained. Finally, the canopy's total volume is calculated by combining the platform and cone volumes. In this investigation, we set the segmented platform thickness (h) to 0.2 m and the thickness of the slice to 0.04 m. Figure 8g depicts the canopy reconstruction effect diagram using a PCH algorithm. The calculation methods are shown in Formulas (4) and (5).

$$S = \frac{1}{2}\sum_{k=1}^{m}(x_k y_{k+1} - x_{k+1} y_k) \tag{4}$$

where m is the number of endpoints and $(x_k y_{k+1})$ and $(x_{k+1} y_k)$ are the plane coordinates of the kth and k + 1th endpoints, respectively.

$$V = \frac{1}{3}\sum_{i=1}^{n-1}\left(S_i + S_{i+1} + \sqrt{S_i S_{i+1}}\right)h_i + \frac{1}{3}S_n h_{n+1} \tag{5}$$

In the formula, $S_i S_{i+1}$ signifies the area of the i, i+1th layer of point cloud slices, n signifies the number of slices, h_i defines the spacing between neighboring slices, h_{n+1} denotes the cone's height, and V denotes the canopy volume.

2.5.6. AS Approach

The AS approach is a classic method for edge extraction. The core idea is to rotate a sphere with radius α inside the specified point set S. When α is sufficiently large, the ball will only roll tangent to the point set's boundary rather than into its interior. At this moment, the points the ball has rolled through come together to create the point set S's boundary (convex hull). Every point could be a border point if α is small enough.

The parameter α influences the fineness of the surface reconstruction results. After reconstructing the experimental fruit trees, it was discovered (Figure 9) that when α = 0.05, the reconstruction effect contained more details and characteristics, making the overall 3D model more realistic and fine. When α = 0.25, there were several flaws, such as insufficient details, particularly for small-scale structures, which could be disregarded, resulting in information loss. When α = 0.5, there was excessive smoothing, which caused blurring of the surface's concave and convex parts as well as the loss of precise branching characteristics. When α = 0.75, an oversimplification developed, resulting in a significant loss of surface details and a structure that was not realistic or exact enough. This research suggested that varying α has a significant impact on the spatial form, compactness, and branching properties of the fruit tree canopy model. Therefore, a value of 0.05 was used in this study (Figure 8e).

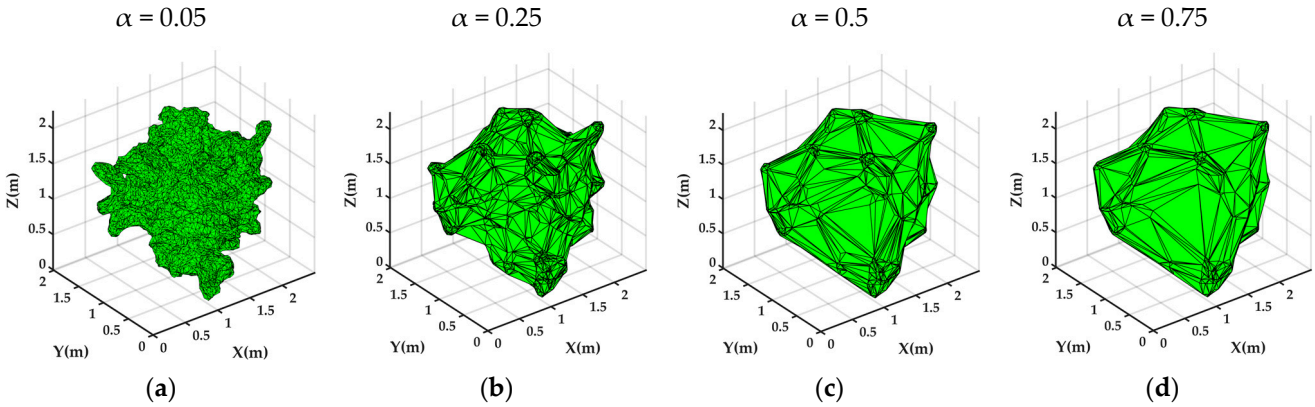


Figure 9. Effect of AS algorithm reconstruction for varying α values.

2.5.7. ASBS Approach

The ASBS algorithm works on a basis identical to that of the CHBS method. The AS algorithm uses α = 0.05 for each segmented point cloud slice, which is the only variation. The value of N was set at 10, as was the case with the CHBS algorithm; the ASBS method results are given in Figure 8f.

2.5.8. DR Approach

Although ASBS performs well in determining canopy volume, due to the varied shapes and sizes of each citrus tree's canopy, slicing the canopy vertically with a consistent thickness has the following disadvantages: it is unable to adapt to the irregular shapes of the canopy, especially at the edges or the top of the canopy, which can lead to over- or under-slicing; slicing the center of the canopy generates too many data points; it does not accurately reflect the complex structures and cavities inside the canopy; and it may ignore some details and properties of the canopy, including branching and density of the foliage; thus, it can comparatively overestimate the volume. Furthermore, it has been established [49] that in the canopy slicing zone, the relatively moderate change in the area of nearby canopy point cloud slices does not necessitate a separate layer. As a result, the slicing method must be adjusted so that it can be used on citrus trees of various shapes and sizes, as well as to compute canopy volume more correctly.

The experimental fruit trees ranged in height from 0.83 m to 2.616 m, and the number of slices per tree was variable, typically between 10 and 30 after adaptive slicing, whereas the citrus trees were dense and morphologically complex, with varying densities of branching structure and distribution. When the fixed value of α = 0.05 was still applied, the problem of volume underestimation occurred due to the smooth surface transition in some locations and the lack of detail in the reconstruction results or the loss of information due to excessive denoising. Using the point cloud's average point spacing as α better reflected the distribution and adapted to point cloud files with different densities, preserving the characteristics of the original point cloud files and reconstructing a volume that was more adaptable, accurate, and reliable.

Cheng et al. [48] developed the triangular mesh growth algorithm and proposed a dynamic threshold improvement α-shape algorithm considering the boundary point cloud density. This algorithm was used with the platform algorithm to compute the volume of the tree, and while it could produce a relatively accurate canopy slice contour, its simple geometric shape reconstruction by using the platform algorithm meant that it was unable to capture the features of complex shapes or scenes with many details, which resulted in inaccurate reconstruction results and a certain number of holes and gaps. In this paper, based on the above features and obstacles, we propose a dynamic slicing and reconstruction algorithm for tree canopy volume (DR). The algorithm flowchart is illustrated in Figure 10. The algorithm's particular phases are listed below:

(1) The canopy point cloud was split into 50 equally spaced slices.
(2) According to the literature [50], when using the α-shape algorithm to construct a contour, a threshold is present α_b; with $\alpha \geq \alpha_b$, the boundary shape formed can include all points from the point set P. The enhanced α-shape approach proposed in the literature [48] iteratively searches for the threshold value α_b of each point cloud slice and obtains the area of the slice's outside geometries under this threshold using the following iterative Formula (6):

$$\alpha_{i+1} = \alpha_i + \Delta\alpha \ (i = 1, 2, \cdots, n) \quad (6)$$

where $\Delta\alpha$ denotes the increment size of each iteration and i denotes the iteration count. In this study, the initial α was set to 0.05, and i was set to 0.1.



Figure 10. Flowchart of the DR algorithm.

(3) Calculate the percentage change in area, *R*, for each neighboring slice with the following formula:

$$R_i = \frac{A_i}{A_{i+1}} - 1 \tag{7}$$

where $\frac{A_i}{A_{i+1}}$ indicates the area ratio of adjacent slices.

(4) Calculate the overall density of each slice using the KNN algorithm:

$$\begin{aligned} \text{localDensity}_i &= \frac{k}{mean(pdist2(\text{Data}_i, \text{Data}_{\text{idx}_i[2:\text{end}]}))} \\ \text{density}_i &= mean(\text{localDensity}) \end{aligned} \tag{8}$$

k is the number of nearest neighbors; here, 10 is used. Data_i is the data point of the ith slice. idx_i is the index of the nearest neighbor of the ith slice. $pdist2(\text{Data}_i, \text{Data}_{\text{idx}_i[2:\text{end}]})$ denotes the distance from the ith slice to its k closest neighbors (excluding itself). The difference between the slice density and the average density is then calculated:

$$\text{D}_i = |density_i - mean(density)| \tag{9}$$

(5) If the percentage change in the area of two neighboring slices R is greater than the average neighboring slice's percentage of area Mean-R or if the difference between the density of two neighboring slices and the average density D is less than the overall average difference Mean-D, the slice is labeled 1; otherwise, it is labeled 0.
(6) If the markers of two neighboring slices are the same, then these two slices are merged; otherwise, the next slice is traversed until all slices are traversed.
(7) The slices are reconstructed by employing the AS algorithm, using the mean point interval distance of the point cloud in the current slice as the α value. The α value is updated until a complete region is generated, and then the volume of that reconstructed region is calculated. The mean point interval distance is as follows: first, the kd-tree structure was utilized to swiftly determine the nearest neighbor of each point in the current slice of the point cloud, and the total distances among all spots were calculated. The average distance was determined by multiplying the total distance by the total number of points in the point cloud.
(8) The total canopy volume was calculated by summing the volumes of all slices.

Figure 8h depicts the performance visualization for crown reconstruction using a DR algorithm, and its performance will be reviewed in Section 3.1.3.

2.6. Algorithm Performance Evaluation Methods

For the accuracy evaluation of the algorithm, the indicators include volumetric results measured by various methods, R^2, regression equation, average number of slices, average reconstructed α value, average slice volume, volume consistency, and average total volume. For the efficiency evaluation, the indicator is the variation in runtime for point cloud files with the same number of points under different methods in the same operating environment. The detailed methodology and analysis of these results will be discussed in Section 3.

3. Experiment and Results

3.1. Canopy Reconstruction

3.1.1. Comparative Analysis of Volumetric Values Using Various Approaches

In this section, we will compare the volume values calculated using different methods. Figure 11 shows a graph comparing the results for 160 citrus tree canopy volume values calculated under eight different methods. This comparison will help us to better understand the advantages and disadvantages of each method and its applicability in practical applications.

Figure 11 shows that the relationships between the volumes measured by the seven algorithms and the MM method are $V_{MM} > V_{CH} > V_{CHBS} > V_{VB} > V_{PCH} > V_{AS} > V_{ASBS}$. Of these, the MM method's calculation of crown volume was greater than that of all PRAs' calculations ($\overline{V}_{MM}$ = 2.72 m^3). This is because the MM method considers the crown to be an oval, whereas the morphology of blood orange fruit trees is frequently complex and irregular. This simplified model accounts for both the external space between the ellipsoid model and the crown's holes and crevices. Consequently, the volume values calculated using the MM method were significantly greater than the canopy's actual volume. Because the CH algorithm treats the fruit tree as a convex polyhedron and accounts for the holes, cracks, and depressions inside the canopy, as well as produces convex packets larger than the canopy contour, it yields the largest calculation result of all PRAs ($\overline{V}_{CH}$ = 2.51 m^3). The result still overestimates the canopy volume ($\overline{V}_{CHBS}$ = 1.87 m^3) even after the CHBS algorithm partially closes the gaps and holes introduced by the CH algorithm. This is because CHBS also has the problem of the nature of the CH algorithm. Although the VB algorithm considers the cubes on the surface of the canopy, because it is difficult to choose cubes of the right size for each fruit tree with a different canopy width and because the cubes' shape and layout cannot be sufficiently adapted to the canopy morphology, its final volume ($\overline{V}_{VB}$ = 1.76 m^3) is larger than the results of the subsequent algorithms. The PCH algorithm can determine three-dimensional canopy information by fully utilizing

external geometric features. It is a simple, fast, and effective method for measuring the volume of a canopy. However, this approach simplifies the canopy morphology to a certain degree and ignores the details of the internal holes, which leads to an increase in the error of volume estimation ($\overline{V}_{PCH}$ = 1.42 m^3). The AS algorithm can accurately extract the boundaries of the canopy point cloud with a reasonable setting of α. The ASBS can eliminate perforations and lacunae in trees with some degree of success, so the AS algorithm calculates a smaller volume ($\overline{V}_{AS}$ = 0.97 m^3), and the ASBS algorithm calculates the smallest volume ($\overline{V}_{ASBS}$ = 0.90 m^3).

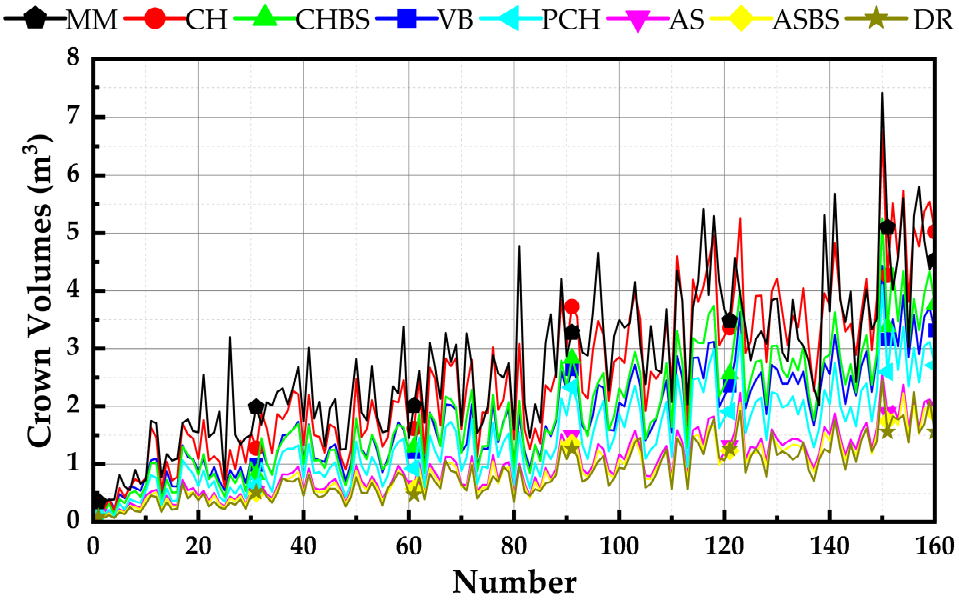


Figure 11. Comparative plot of volumetric values of 160 blood orange trees measured by the MM method and seven PRAs. Node: manual method (MM); convex hull (CH); convex hull by slices (CHBS); voxel-based (VB); platform convex hull (PCH); alpha-shape (AS); alpha-shape by slices (ASBS); dynamic slicing and reconstruction (DR) algorithms.

3.1.2. Comparative Analysis of R^2 and Regression Coefficients for Various Approaches

The volume fits calculated by the eight methods are shown in Table 3 to investigate the associations between the different methods, with the R^2 values of MM and PRAs being relatively low, ranging from 0.802 to 0.854, and the R^2 values of the seven types of PRAs ranging from 0.962 to 0.999. The R^2 and regression equation for various approaches in Table 3 agree with the quantitative connections in Figure 11.

A boost in the variation in regression coefficients between the V_{MM} and the volume measurements of the other methods implies a boost in the variation in the V_{MM} and the volume measured by the other methods. The V_{MM}'s linear fit R^2 to other methods' volume measurements decreases as the volume discrepancy increases. This is because the ellipsoid model takes into account both the perforations and lacunae inside the trees as well as the exterior space between the canopy and the oval model, resulting in a significant overestimation of canopy volume. The CH algorithm removed some of the outside area surrounding the canopy and the ellipsoid model, the CHBS algorithm removed some of the holes and gaps, and the subsequent algorithms all progressively removed more holes and gaps to some degree to optimize the details of extracting the canopy boundaries. The changes in the regression coefficients and R^2 that were previously discussed are thus the result of the continuous growth in the disparity between the measured MM and PRAs.

Table 3. R^2 and regression equation for various approaches.

Eq./R^2	V_{MM}	V_{CH}	V_{CHBS}	V_{VB}	V_{PCH}	V_{AS}	V_{ASBS}	V_{DR}
V_{MM}		$y = 0.884x + 0.495$	$y = 1.124x + 0.615$	$y = 1.345x + 0.341$	$y = 1.460x + 0.642$	$y = 2.199x + 0.575$	$y = 2.353x + 0.600$	$y = 2.346x + 0.750$
V_{CH}	0.854		$y = 1.284x + 0.109$	$y = 1.536x - 0.201$	$y = 1.664x + 0.145$	$y = 2.516x + 0.061$	$y = 2.690x + 0.091$	$y = 2.678x + 0.265$
V_{CHBS}	0.827	0.989		$y = 1.195x - 0.242$	$y = 1.297x + 0.025$	$y = 1.963x - 0.042$	$y = 2.097x - 0.017$	$y = 2.088x + 0.118$
V_{VB}	0.819	0.979	0.989		$y = 1.078x + 0.233$	$y = 1.646x + 0.161$	$y = 1.759x + 0.183$	$y = 1.743x + 0.304$
V_{PCH}	0.820	0.977	0.995	0.989		$y = 1.509x - 0.048$	$y = 1.611x - 0.027$	$y = 1.602x + 0.077$
V_{AS}	0.802	0.962	0.978	0.994	0.982		$y = 1.068x + 0.013$	$y = 1.053x + 0.090$
V_{ASBS}	0.805	0.964	0.977	0.994	0.980	0.999		$y = 0.985x + 0.072$
V_{DR}	0.794	0.948	0.962	0.968	0.962	0.965	0.964	

The lower R^2 of the CH algorithm compared to that of the other algorithms suggests that its predictive power is relatively weak, and the larger intercepts of the regression equations of the CH and CHBS algorithms compared to the smaller intercepts of the other algorithms imply that the CH and CHBS algorithms overestimate the volume of the tree crowns more than do the other algorithms. The VB algorithm is a voxel-based algorithm that does not compute a cube's volume when there is no point cloud present, which is why V_{CHBS} is larger than V_{VB}. The PCH algorithm fits the data well, with moderate slopes and minor intercepts in the fitted equations and a significant correlation with the AS method, indicating that its estimated volumes are relatively accurate. The CH and AS algorithms have substantial differences in terms of reconstruction effectiveness and accuracy. The CH algorithm simplifies the canopy shape and ignores internal details and holes. The AS algorithm, on the other hand, can generate canopy shapes with varying degrees of fineness based on the parameter α. This algorithm is more sensitive to external details and can accurately reconstruct the canopy shape. The intercepts of the AS and ASBS algorithms with the other algorithms are small (between 0.013 and 0.91), and only with the VB algorithm are the intercepts the largest (0.161 and 0.183), which suggests that the VB algorithm does not represent the genuine fruit tree structures with the details of the contours very well using small cubes and overestimates the volume of the canopy. The R^2 values for the AS and ASBS are 0.999, and both the intercepts and the slopes are very small, indicating that they are strongly correlated; since the ASBS has the smallest volume, its slope (1.068–2.690) is greater than that of all the other algorithms.

3.1.3. Comparative Analysis of DR Algorithms

Figure 1b shows that the natural round-headed type of citrus tree will have branches that naturally droop when fruiting, with fruit moving toward the bottom and central sections of the canopy, with the lower part usually having more fruit and branches and leaves concentrated in the elevated and central sections of the tree. Because the experimental fruit tree was a blood orange fruit tree that was grafted and planted in 2021 and is still in the process of cultivating its second layer, the majority of the top is covered with new, unfruitful branches, and it is quite sparse. The DR algorithm dynamically merges slices by taking into account the ratio of area change and density difference of neighboring slices: the change in the area of slices tends to reflect the actual shape and growth characteristics of the canopy; if the ratio of area change of a slice is larger than the average area change ratio, it means that the canopy in that part is growing more vigorously; these areas may be

new-growing branches or foliage or rapidly growing fruits; if a slice's density difference is less than the average density difference, this suggests that the health of that portion of the canopy is more stable and that the growth is more balanced.

Following the analysis of the agronomic traits, the side-by-side reconstruction view of the DR algorithm (Figure 12) shows that the dynamic slices more thoroughly consider the area and density characteristics of the slices, making it easier to identify the areas of dense foliage and branches, areas of concentrated fruit, and areas of sparse density in the roots and tops of trees. The best α values for these regions are automatically determined by the constant iteration of point spacing α values: for the branch- and fruit-rich regions, a smaller α value is used to refine the reconstruction (0.0244–0.0775), which better captures the detailed contour and structure of the branches, leaves, and fruits, making the model more structurally realistic; for the root and top slices of the tree, which are sparsely populated with branches and fruits, a slightly larger α value is used for a looser reconstruction (0.1161–0.3306), which is able to capture the overall shape and structure, resulting in a smoother and more stable overall contour of the canopy.

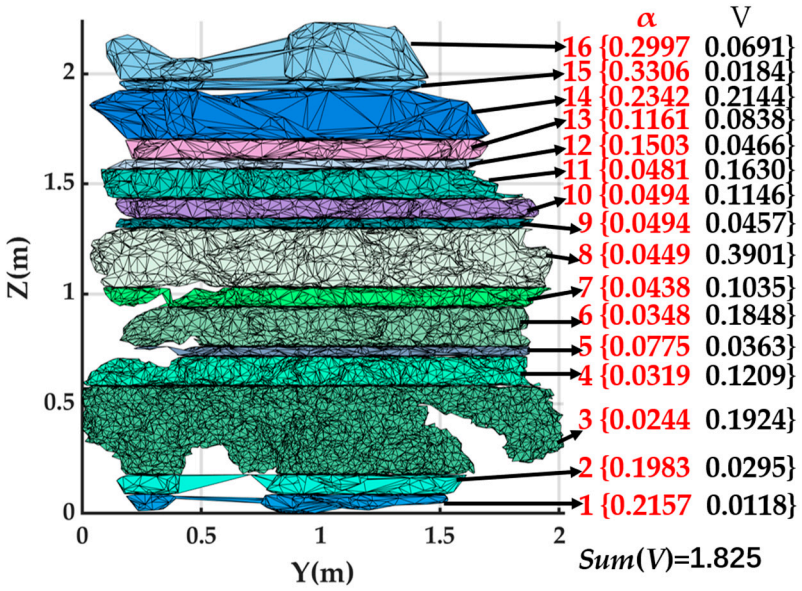


Figure 12. Lateral angle of the reconstruction using the DR algorithm, different colors represent different slices. Note: α, the α-value used for AS reconstruction from the slice; $Sum(V)$ signifies the total volume of the canopy; V, sliced point cloud volume.

Because the true volume of the canopy is not available, we used the ASBS algorithm, which performs better than the other six algorithms; the PCH algorithm, which is widely applicable; and the CHBS algorithm, which also uses a slicing method, for comparison with our proposed algorithm. We used the four methods to compute the average number of slices per tree ($\overline{n}$), the average value of α per slice ($\overline{\alpha}$), the average value of volume consistency ($\overline{VC}$), and the average value of volume per slice ($\overline{v}$) for the 160 blood orange fruit trees. The volume consistency of a tree is obtained by multiplying the standard deviation of the slice volume by the mean value of the slice volume as follows:

$$\text{volumeConsistency} = \frac{\sqrt{\frac{1}{n}\sum_{m=1}^{n}(V_m - V_{\text{ave}})^2}}{V_{\text{ave}}} \tag{10}$$

where n represents the number of slices, V_m denotes the current slice volume, and V_{ave} denotes the average slice volume.

As shown in Table 4, both CHBS and ASBS used a fixed number of slices (10) in each tree and reconstructed each slice in the same way, resulting in extremely consistent volume

consistency (0.556 and 0.665). However, the growth pattern of citrus trees is inherently inhomogeneous, and the density and volume of each part (for example, the root, middle, and top of the canopy) vary greatly, which CHBS and ASBS did not account for in the stratification, resulting in reconstructed models that were too consistent and stable to accurately represent citrus tree growth. Because the PCH divides the circular platform at a height of 0.4 m, it dynamically stratifies the citrus trees to some extent. Specifically, it divides each tree's top into a conical shape and platform slicing of the remaining area according to the height of the canopy. As a result, its volume consistency is closer to the citrus distribution pattern (0.710) than that of ASBS and CHBS, but because it still relies on a basic geometric model to calculate volume, the volume that is obtained will be on the large side and will not be able to adequately remove the holes and gaps. DR dynamically stratified each fruit tree and used different a-values for different parts of the tree. According to the results (1.532), DR better represented the growth characteristics and morphological features of various parts of the citrus tree (e.g., canopy densities, branch/fruit distributions), as well as more continuous and smoother reconstruction results and alpha shapes that better matched the original data to obtain a more accurate canopy volume.

Table 4. Comparative analysis of DR with CHBS, PCH, and ASBS.

Algorithm	$\overline{n}$	$\overline{\alpha}$	$\overline{v}$	$\overline{VC}$	$\overline{V}$
CHBS	10	*No*	0.187	0.556	1.872
PCH	5	*No*	0.254	0.709	1.339
ASBS	10	0.05	0.09	0.664	0.901
DR	13.806	0.085	0.065	1.532	0.84

Note: the average number of slices per tree, $\overline{n}$; the average value of α per slice, $\overline{\alpha}$; the average value of volume consistency, $\overline{VC}$; and the average value of volume per slice, $\overline{v}$.

According to the density and shape of the point cloud files, DR dynamically modifies the thickness of the slices and the α-value to more closely resemble the real canopy situation when processing the point cloud data, effectively eliminating holes and gaps. As shown in Figure 11, the volumetric values measured by the DR on the 160 experimental trees tended to be stable, and the volumetric mean value was lower than that of all six other algorithms (VDR = 0.84). Table 3 shows that DR has more significant slopes and intercepts in the regression equations with other algorithms (the intercepts are more significant than the effects of PCH, AS, and ASBS examined in the previous section). Additionally, the previous analysis revealed that the R^2 value of the fit with MM is lower for algorithms that are more accurate because ellipsoidal models differ significantly from the actual volume of the crown, which ignores the fact that every tree is distinct, with varying fruit distributions, branch and leaf densities, and gaps and holes between canopies (which the CH algorithm does as well). The R^2 for DR and the other algorithms is approximately 0.96, indicating that the volume derived by the algorithm is stable and that the goodness of fit is satisfactory. The R^2 is lower than that of the ASBS and other algorithms because DR begins with the canopy's internal structure, using the correlation between density and area to dynamically slice the slices and iteratively searching for the optimal a-value for reconstruction based on the distribution of branches, leaves, and fruits in each slice. Conventional algorithms all utilize a simple uniformized slicing and reconstruction approach rather than dynamically correcting changes from the underlying structure of the canopy, as does DR; hence, R^2 is greater among numerous other algorithms, while DR is lower. This information is crucial for analyzing citrus tree growth patterns and forecasting fruit supply in the future.

3.1.4. Comparative Analysis of Algorithm Runtimes for Various Approaches

MATLAB R2023a software was used for running seven PRA programs on a Dell computer (Intel Core i9-12900 @2.40 GHz processor, Samsung DDR5 4800 MHz 16 GB × 2 RAM, 512 GB SSD). All other background processes were closed during the program execution. The running times of several algorithms are displayed in Figure 10.

Figure 13 illustrates the link between the running times of the seven volume-finding algorithms as follows: $T_{VB} < T_{CHBS} < T_{CH} < T_{PCH} < T_{ASBS} < T_{AS} < T_{DR}$. VB employs a simple data structure (3D labeled array) and a straightforward traversal technique with low processing complexity. In the loop, only one traversal of the point cloud files is performed, and each point is assigned to the appropriate rectangle. Due to its simplicity, this procedure takes the least time to complete ($\overline{T}_{VB}$ = 0.126). Although CHBS requires an additional slicing phase, the small amount of data in each slice results in a very fast computation of the CH. Sliced data can often make greater use of the computer's memory architecture, such as caches, perhaps leading to faster computations. Because the sliced dataset is smaller, it fits more easily into the cache and allows for faster data reading and manipulation during processing ($\overline{T}_{CHBS}$ = 0.145). In comparison, applying the CH method ($\overline{T}_{CH}$ = 0.2) directly to the complete point cloud data will have a higher computational complexity because it needs to process a larger quantity of data; hence, the CH takes slightly longer than the CHBS. Similarly, the ASBS algorithm ($\overline{T}_{ASBS}$ = 1.294) outperforms the AS algorithm ($\overline{T}_{AS}$ = 1.457) according to the same principle. Slicing also streamlines the calculation process and minimizes the overall computational effort when considering hardware environments such as processor multicore architecture and memory access efficiency. Because the DR algorithm executes many lookup and iteration operations, it is the longest running algorithm among the PRAs ($\overline{T}_{DR}$ = 11.429).

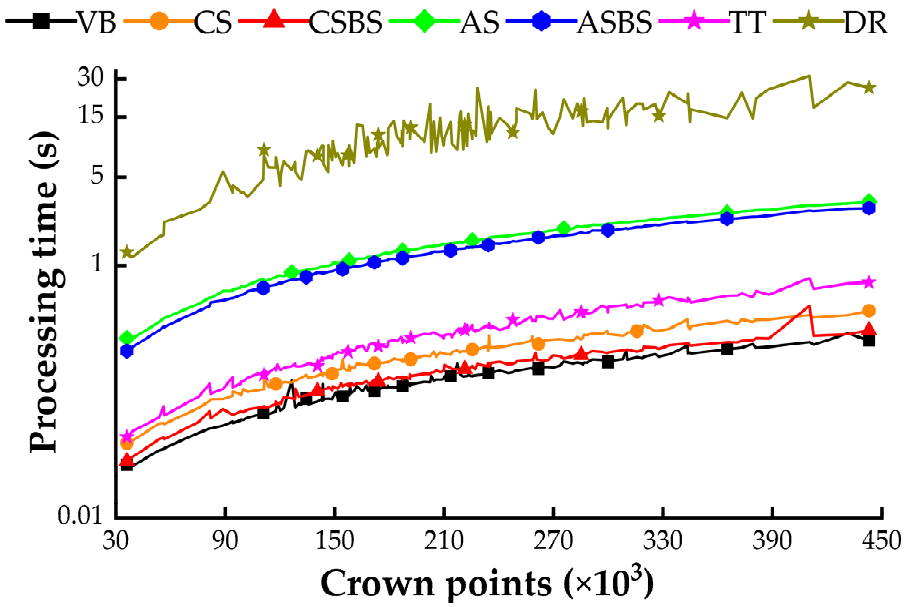


Figure 13. Comparison plot of run times for seven PRAs measuring 160 blood orange trees.

4. Discussion

4.1. Discussion of the Number of Slices

Based on earlier investigations [32,46] on the number of slices, five distinct numbers of slices (N = 10, 20, 30, 40, and 50) were selected for the discussion of how the number of slices affects the outcomes of ASBS and CHBS reconstructions in terms of both volume and runtime.

4.1.1. CHBS

Figure 14 demonstrates how the number of slices affects the reconstructed volume in the CHBS. The percentages of perforations and lacunae eliminated by the original CH algorithm were 26.4%, 31.3%, 33.7%, 35.3%, and 36.5%, respectively, when varying numbers of slices were used (N = 10, 20, 30, 40, 50). As the number of slices increased, the regression coefficients (slope and intercept) between CHBS and CH slowly increased, and the weak

change in R^2 suggested that increasing the number of slices from the interval of 20–50 did not significantly improve CH.

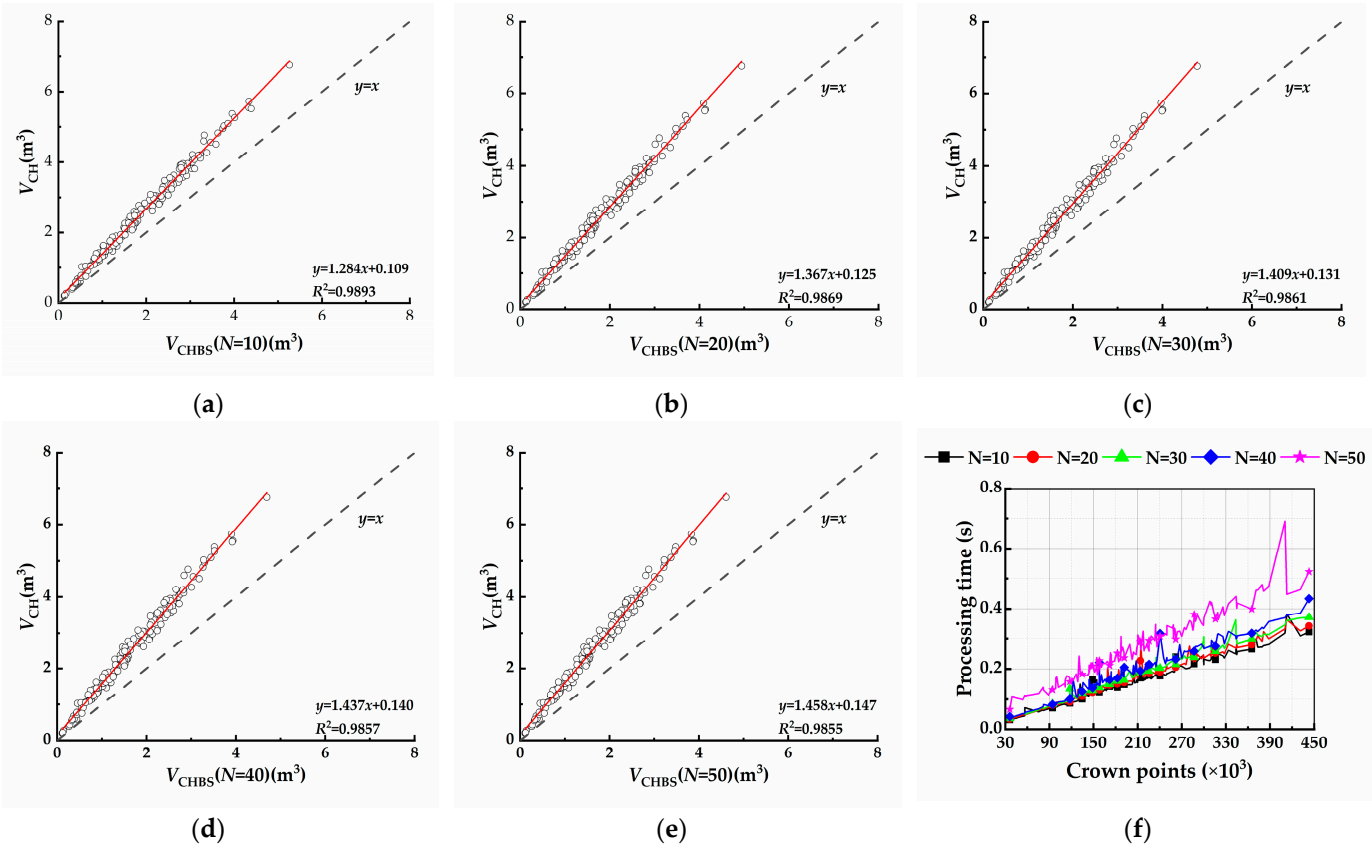


Figure 14. Impact of the number of slices (N) on the reconstruction volume in the CHBS approach. (**a**) N is set to 10; (**b**) 20; (**c**) 30; (**d**) 40; (**e**) 50. (**f**) Impact of various numbers of slices on the running time of the CHBS approach.

Figure 14f shows that when the number of processed point clouds increases, the CHBS algorithm running time increases progressively. The runtime climbs by 0.02 s for every 10 extra slices in terms of the number of slices and by 0.07 s when the number of slices climbs from 40 to 50. According to this linear relationship, the computational cost of the algorithm increases with the number of slices, and this increase becomes more noticeable as the number of slices increases. Fernández et al. [51] study revealed that applying the CHBS algorithm reduced the overestimation that the CH approach caused, while only slightly increasing processing time. This matches the findings of our experiment.

4.1.2. ASBS

Figure 15 depicts the effect of the number of slices on the reconstructed volume in the ASBS. The percentages of perforations and lacunae eliminated by the original AS algorithm were 8.0%, 16.1%, 23.7%, 30.7%, and 36.9%, respectively, when varying numbers of slices were used (N = 10, 20, 30, 40, 50). The trends and reasons for the regression coefficients and R^2 values of V_{AS} and V_{ASBS} were identical in terms of V_{CH} and V_{CHBS}, but the regression coefficients of ASBS versus AS increased more with the number of slices, and the R^2 values decreased faster, indicating that the AS algorithm was more successful at eliminating perforations and lacunae than the CH algorithm. Liu et al. [32] experiments with the ASBS algorithm demonstrated this as well.

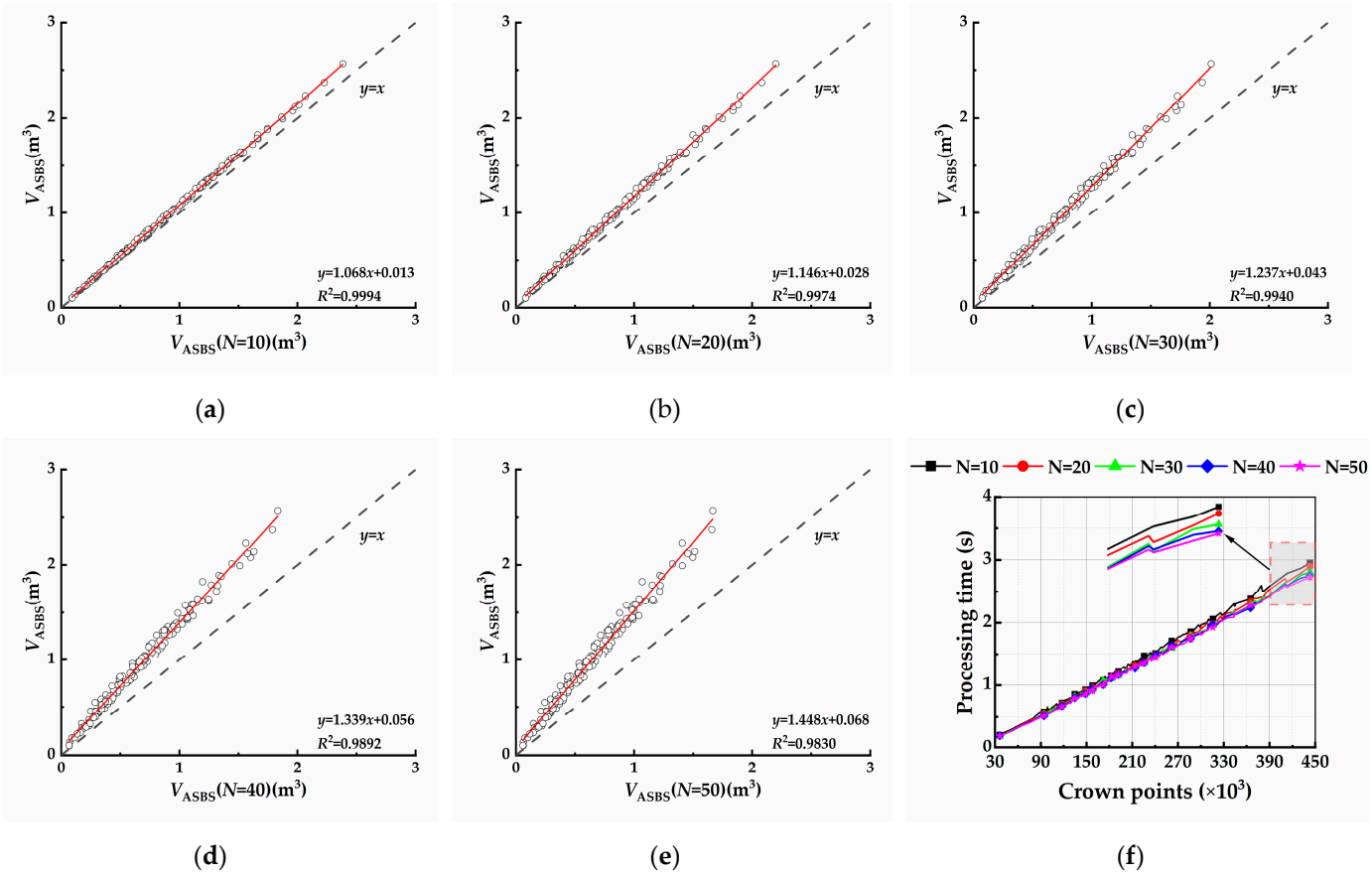


Figure 15. Impact of the number of slices (N) on the reconstruction volume in the ASBS approach. (**a**) N is set to 10; (**b**) 20; (**c**) 30; (**d**) 40; (**e**) 50. (**f**) Impact of various numbers of slices on the running time of the ASBS approach.

With regard to execution time, $\overline{T}_{ASBS}$ takes 2 s more than the $\overline{T}_{CHBS}$ algorithm in processing the same number of points. When the number of points computed increases, the running time shows a stable linear increase, indicating that the execution time of the ASBS approach remains constant across a range of point cloud file sizes. Interestingly, as the number of slices increases, the running time of the ASBS algorithm decreases, and this decrease becomes increasingly obvious as the number of points increases (Figure 15f). We predict that this is associated with the peculiarities of citrus tree point cloud data as well as the working concept of AS. Citrus tree point cloud data have a high density and volume, and increasing the number of slices reduces the size of individual slices, reducing the processing time per slice. Furthermore, because citrus tree point cloud data contain some overlap and continuity, increasing the number of slices reduces the degree of overlap between slices and unnecessary calculations, resulting in increased efficiency. AS typically reconstructs surfaces by identifying local geometric structures in the point cloud data and then utilizes the geometric structures to generate smooth surface representations. Increasing the number of slices will provide more local geometric information, which will help to reconstruct the surface more accurately, thus reducing the time for subsequent processing. This is also related to the possible optimization of the hardware environment and MATLAB version, as mentioned before.

4.2. Discussion on the Application Scenarios for Each Algorithm

When selecting relevant algorithms, different application scenarios and needs must be considered to provide valuable data support and decision-making references for connected businesses. We discuss this phenomenon after a thorough analysis of the reconstruction effect, algorithm principle, volume, and running time.

The MM volume is significantly greater than the real volume of the tree canopy; this approach is laborious and complicated, and it is weaker than a point cloud-based approach. CHBS reduces some of the flaws and gaps of the CH method, making it less significant than overestimation, and it also keeps the fruit tree shape contour while improving the runtime, with an average runtime that is only 0.02 s slower than that of the VB approach. In the case of real-time obstacle avoidance in agricultural robots, which requires quick and precise volume and contour information from the tree canopy, CHBS combines fast slice-volume computation with an accurate convex bagging technique, making it an excellent candidate. The VB can determine the volume of tree crowns rapidly and precisely, making it useful for measuring leaf area and analyzing plant health. It also has uses in urban greening planning and forest resource management. The PCH algorithm has a strong mathematical foundation and reliability, is resistant to data noise and interference, and the computational process is relatively simple, resulting in high computational efficiency and certain advantages in large-scale data processing and real-time monitoring. It can be used to examine the development and canopy structure of forest vegetation, as well as to offer data for forest preservation and resource utilization. ASBS is an optimization of the AS algorithm that produces more accurate results than previous algorithms and is appropriate for large-scale spray volume estimation. DR can better describe the canopy shape and density distribution; by using the average point spacing as the α-value, the reconstruction method can better adapt to the localized properties of the point cloud, resulting in improved accuracy and efficiency. This is especially useful in the reconstruction of citrus trees with complex shapes and wide density variations. It can also be used to assess crop growth status and the exact volume of the plant canopy, allowing agricultural producers to adjust management measures such as irrigation and fertilization in real time to increase crop yield and quality.

In related study, Yu et al. [52] used the slicing method to improve the projected convex hull by applying it to the volume calculation of regular contours (water bottles, glass) and irregular contours (toy artwork), and discovered that the improved slicing algorithm greatly improves accuracy and has high stability, indicating that the slicing method is an effective improvement over traditional algorithms, which is consistent with our findings. Yan et al. [46] used the MM, VB, CH, CHBS, and AS algorithms to reconstruct roadside trees, and found that the MM, CH, and CHBS algorithms consistently yielded larger volume values than any of the other algorithms, and that VB was the fastest to compute, which is also consistent with our findings.

5. Conclusions

This study presents a DR algorithm for citrus tree canopy reconstruction and volume estimation, which was analyzed along with six mainstream algorithms. The specific research is summarized below:

(1) A collection of processing procedures is offered for three-dimensional reconstruction designed to use handheld laser scanners on large-scale citrus farms. Detailed procedures and parameters for the reconstruction of pretreatment are provided, especially for high ridges and deep furrows for soil bundling in southern hilly areas.

(2) Based on reconstruction effects and efficiency, the algorithms are categorized into three groups: CH and CHBS: Overestimate results, suitable for obstacle avoidance in agricultural robots with real-time sensing; VB and PCH: Conservative approaches, effective for crops with uniform distribution and simple structures; AS, ASBS, and DR: Reliable conservative methods, ideal for large-scale, precise spraying volume estimation and fertilization decision guidance.

(3) When N = 10, the number of slices significantly affected the volumetric values calculated by the CH algorithm, and the running time was reduced. However, as the number of slices increased, this effect diminished, and the running time increased. Therefore, CHBS with N = 10 is recommended for citrus tree reconstruction. The AS algorithm showed a considerable and steady effect on volumetric values with an increasing number of slices, and adding slices enhanced operational efficiency. This

indicates that slicing-based optimization of the AS algorithm is useful for citrus tree reconstruction.

(4) A dynamic slicing and reconstruction algorithm was developed to accurately determine the volume of the citrus canopy. This algorithm effectively removes holes and gaps in the canopy, resulting in a more accurate reconstruction model, aiding in the analysis of agronomic traits.

Although the DR algorithm effectively calculates canopy volume, further optimization is needed for its applicability and runtime in various scenarios. Efficient preprocessing and segmentation of point cloud data and integrating different sensor data for comprehensive canopy characterization remain research challenges. Future research should focus on improving algorithms for specific operational environments, developing real-time processing algorithms, and investigating multi-source data fusion, such as integrating with inspection vehicles for yield estimation [53] and fusing with image data for volume prediction [54]. These improved algorithms can be integrated into intelligent agricultural management systems to support fine management, precision fertilization, and pest control applications.

Author Contributions: Conceptualization, W.L. and Y.Z.; Data curation, W.L., Z.H. and H.W.; Formal analysis, W.L., H.W. and Z.B.; Funding acquisition, Y.Z.; Investigation, W.L., B.T. and Q.Y.; Methodology, W.L., B.T. and Y.Z.; Project administration, W.L. and Y.Z.; Resources, W.L. and Q.Y.; Software, W.L., B.T. and Z.H.; Supervision, Y.Z.; Validation, W.L. and Z.B.; Visualization, W.L.; Writing—original draft, W.L. and Y.Z.; Writing—review and editing, W.L. and Y.Z. All authors have read and agreed to the published version of the manuscript.

Funding: The National Natural Science Foundation of China (31972991), the earmarked fund for the China Agriculture Research System (CARS-26), the Key Research and Development Project of Southwest University Pilot Plan (SWU-XDZD22004), and the Technology Innovation and Application Development Project in Chongqing (CSTB2023TIAD-LUX0001).

Data Availability Statement: The datasets presented in this article are not readily available because the data are part of an ongoing study.

Conflicts of Interest: The authors declare no conflicts of interest.

References

1. Wang, T.; Li, J.; He, L.; Deng, L.; Yongqiang, Z.; Yi, S.; Xie, R.; Lyu, Q. Citrus canopy volume estimation using UAV oblique photography. *Int. J. Precis. Agric. Aviat.* **2021**, *1*, 22–28. [CrossRef]
2. Guofu, Z.; Min, Y. The achievements, problems and suggestions of the development of citrus export trade in China. *South China Fruits* **2024**, *53*, 234–242.
3. Pommerening, A.; Sánchez Meador, A.J. Tamm review: Tree interactions between myth and reality. *For. Ecol. Manag.* **2018**, *424*, 164–176. [CrossRef]
4. Li, F.; Cohen, S.; Naor, A.; Shaozong, K.; Erez, A. Studies of canopy structure and water use of apple trees on three rootstocks. *Agric. Water Manag.* **2002**, *55*, 1–14. [CrossRef]
5. Pereira, A.R.; Green, S.; Villa Nova, N.A. Penman–Monteith reference evapotranspiration adapted to estimate irrigated tree transpiration. *Agric. Water Manag.* **2006**, *83*, 153–161. [CrossRef]
6. Villalobos, F.J.; Testi, L.; Hidalgo, J.; Pastor, M.; Orgaz, F. Modelling potential growth and yield of olive (*Olea europaea* L.) canopies. *Eur. J. Agron.* **2006**, *24*, 296–303. [CrossRef]
7. Zaman, Q.; Schumann, A.; Hostler, H. Estimation of citrus fruit yield using ultrasonically-sensed tree size. *Appl. Eng. Agric.* **2006**, *22*, 39–44. [CrossRef]
8. Primo-Capella, A.; Molina-Nadal, M.D.; Catalá-Senent, L.; de Miguel-Moreno, A.; Forner-Giner, M.Á.; Martínez-Cuenca, M.-R. Response to Deficit Irrigation of 'Orogrande' Mandarin Grafted onto Different Citrus Rootstocks in Spain. *Horticulturae* **2024**, *10*, 37. [CrossRef]
9. Guo, S.; Chen, C.; Du, G.; Yu, F.; Yao, W.; Yubin, L. Evaluating the use of unmanned aerial vehicles for spray applications in mountain Nanguo pear orchards. *Pest Manag. Sci.* **2024**, *80*, 3590–3602. [CrossRef]
10. Abbas, I.; Liu, J.; Faheem, M.; Noor, R.S.; Shaikh, S.A.; Solangi, K.A.; Raza, S.M. Different sensor based intelligent spraying systems in Agriculture. *Sens. Actuators A Phys.* **2020**, *316*, 112265. [CrossRef]
11. Kolmanič, S.; Strnad, D.; Kohek, Š.; Benes, B.; Hirst, P.; Žalik, B. An algorithm for automatic dormant tree pruning. *Appl. Soft Comput.* **2021**, *99*, 106931. [CrossRef]
12. Ye, X.-J.; Sakai, K.; Asada, S.I.; Sasao, A. Inter-Relationships Between Canopy Features and Fruit Yield in Citrus as Detected by Airborne Multispectral Imagery. *Trans. ASABE* **2008**, *51*, 739–751. [CrossRef]

13. Marín-Buzón, C.; Pérez-Romero, A.; Tucci-Álvarez, F.; Manzano-Agugliaro, F. Assessing the Orange Tree Crown Volumes Using Google Maps as a Low-Cost Photogrammetric Alternative. *Agronomy* **2020**, *10*, 893. [CrossRef]
14. Krajewski, A.; Schumann, A.; Ebert, T.; Oswalt, C.; Ferrarezi, R.; Waldo, L. Management of Citrus Tree Canopies for Fresh-Fruit Production. *EDIS* **2021**, *2021*. [CrossRef]
15. Mu, Y.; Fujii, Y.; Takata, D.; Zheng, B.; Noshita, K.; Honda, K.; Ninomiya, S.; Guo, W. Characterization of peach tree crown by using high-resolution images from an unmanned aerial vehicle. *Hortic. Res.* **2018**, *5*, 74. [CrossRef] [PubMed]
16. De-Yu, H.; Xue-Feng, L.; Shao-Lan, H.; Rang-Jin, X.; Chun, Q.; Qiang, L.; Shi-Lai, Y.; Yong-Qiang, Z.; Lie, D. Effect of plant canopy transformation on chlorophyll fluorescence characteristics and fruit yield and quality in closed citrus orchard. *Sci. Agric. Sin.* **2017**, *50*, 1734–1746.
17. Miranda-Fuentes, A.; Llorens, J.; Gamarra-Diezma, J.L.; Gil-Ribes, J.A.; Gil, E. Towards an optimized method of olive tree crown volume measurement. *Sensors* **2015**, *15*, 3671–3687. [CrossRef]
18. Zheng, Y.; Deng, L.; He, S.; Zhou, Z.; Yi, S.; Mao, S.; Zhao, X. Effects of seven rootstocks on tree growth, yield and fruit quality of 'Hamlin'sweet orange in south China. *Acta Hortic. Sin.* **2010**, *37*, 532–538.
19. Lee, K.; Ehsani, R. A laser scanner based measurement system for quantification of citrus tree geometric characteristics. *Appl. Eng. Agric.* **2009**, *25*, 777–788. [CrossRef]
20. Li, P.; Zhang, M.; Wang, T.; Zheng, Y.; Yi, S.; Lü, Q. Real-time estimation of citrus canopy volume based on laser scanner and irregular triangular prism module method. *Sci. Agric. Sin.* **2019**, *52*, 4493–4504.
21. Dong, X.; Zhang, Z.; Yu, R.; Tian, Q.; Zhu, X. Extraction of information about individual trees from high-spatial-resolution UAV-acquired images of an orchard. *Remote Sens.* **2020**, *12*, 133. [CrossRef]
22. Jurado, J.M.; Ortega, L.; Cubillas, J.J.; Feito, F. Multispectral mapping on 3D models and multi-temporal monitoring for individual characterization of olive trees. *Remote Sens.* **2020**, *12*, 1106. [CrossRef]
23. Dong, W.; Roy, P.; Isler, V. Semantic mapping for orchard environments by merging two-sides reconstructions of tree rows. *J. Field Robot.* **2020**, *37*, 97–121. [CrossRef]
24. Yin, Y.; Liu, G.; Li, S.; Zheng, Z.; Si, Y.; Wang, Y. A Method for Predicting Canopy Light Distribution in Cherry Trees Based on Fused Point Cloud Data. *Remote Sens.* **2023**, *15*, 2516. [CrossRef]
25. Yu, L.; Hong, T.; Zhao, Z.; Huang, J.; Zhang, L. 3D-reconstruction and volume measurement of fruit tree canopy based on ultrasonic sensors. *Trans. Chin. Soc. Agric. Eng.* **2010**, *26*, 204–208.
26. Maghsoudi, H.; Minaei, S.; Ghobadian, B.; Masoudi, H. Ultrasonic sensing of pistachio canopy for low-volume precision spraying. *Comput. Electron. Agric.* **2015**, *112*, 149–160. [CrossRef]
27. Zhang, J.; Xie, T.-J.; Wei, X.-N.; Wang, Z.-K.; Liu, C.-T.; Zhou, G.-S.; Wang, B. Estimation of feed rapeseed biomass based on multi-angle oblique imaging technique of unmanned aerial vehicle. *Acta Agron. Sin.* **2021**, *47*, 1816–1823.
28. Zhu, B.; Li, M.; Liu, F.; Jia, A.; Mao, X.; Guo, Y. Modeling of canopy structure of field-grown maize based on UAV images. *Trans. Chin. Soc. Agric. Mach* **2021**, *52*, 170–177.
29. Rosell, J.; Sanz, R. A review of methods and applications of the geometric characterization of tree crops in agricultural activities. *Comput. Electron. Agric.* **2012**, *81*, 124–141. [CrossRef]
30. Sultan Mahmud, M.; Zahid, A.; He, L.; Choi, D.; Krawczyk, G.; Zhu, H.; Heinemann, P. Development of a LiDAR-guided section-based tree canopy density measurement system for precision spray applications. *Comput. Electron. Agric.* **2021**, *182*, 106053. [CrossRef]
31. Xu, W.-H.; Feng, Z.-K.; Su, Z.-F.; Xu, H.; Jiao, Y.-Q.; Deng, O. An automatic extraction algorithm for individual tree crown projection area and volume based on 3D point cloud data. *Spectrosc. Spectr. Anal.* **2014**, *34*, 465–471.
32. Liu, X.; Wang, Y.; Kang, F.; Yue, Y.; Zheng, Y. Canopy parameter estimation of citrus grandis var. Longanyou based on Lidar 3d point clouds. *Remote Sens.* **2021**, *13*, 1859. [CrossRef]
33. Chakraborty, M.; Khot, L.R.; Sankaran, S.; Jacoby, P.W. Evaluation of mobile 3D light detection and ranging based canopy mapping system for tree fruit crops. *Comput. Electron. Agric.* **2019**, *158*, 284–293. [CrossRef]
34. Wang, W.J.; Yang, H.J.; Feng, Z.K. Tridimensional green biomass measurement for trees using 3-D laser scanning. *Nongye Jixie Xuebao = Trans. Chin. Soc. Agric. Mach.* **2013**, *44*, 229–233.
35. Quan, C.; Songlin, X.; Mei, Y.; Jinhui, H. Effect of Different Pruning on Growth and Fruit Bearing of 'Blood Orange No.8'. *Mol. Plant Breed.* **2023**, 1–15.
36. Zeng, Q.; Mao, J.; Li, X.; Liu, X. Planar-fitting filtering algorithm for LIDAR points cloud. *Geomat. Inf. Sci. Wuhan Univ.* **2008**, *33*, 25–28.
37. Fischler, M.A.; Bolles, R.C. Random sample consensus: A paradigm for model fitting with applications to image analysis and automated cartography. *Commun. ACM* **1981**, *24*, 381–395. [CrossRef]
38. Zhang, W.; Qi, J.; Wan, P.; Wang, H.; Xie, D.; Wang, X.; Yan, G. An Easy-to-Use Airborne LiDAR Data Filtering Method Based on Cloth Simulation. *Remote Sens.* **2016**, *8*, 501. [CrossRef]
39. Hojjatoleslami, S.; Kittler, J. Region growing: A new approach. *IEEE Trans. Image Process.* **1998**, *7*, 1079–1084. [CrossRef]
40. Hu, C.; Pan, Z.; Zhong, T. Leaf and wood separation of poplar seedlings combining locally convex connected patches and K-means++ clustering from terrestrial laser scanning data. *J. Appl. Remote Sens.* **2020**, *14*, 018502. [CrossRef]

41. Ferrara, R.; Virdis, S.G.; Ventura, A.; Ghisu, T.; Duce, P.; Pellizzaro, G. An automated approach for wood-leaf separation from terrestrial LIDAR point clouds using the density based clustering algorithm DBSCAN. *Agric. For. Meteorol.* **2018**, *262*, 434–444. [CrossRef]
42. Gamal, A.; Wibisono, A.; Wicaksono, S.B.; Abyan, M.A.; Hamid, N.; Wisesa, H.A.; Jatmiko, W.; Ardhianto, R. Automatic LIDAR building segmentation based on DGCNN and euclidean clustering. *J. Big Data* **2020**, *7*, 102. [CrossRef]
43. Cao, Y.; Wang, Y.; Xue, Y.; Zhang, H.; Lao, Y. FEC: Fast Euclidean Clustering for Point Cloud Segmentation. *Drones* **2022**, *6*, 325. [CrossRef]
44. Rusu, R.B.; Marton, Z.C.; Blodow, N.; Dolha, M.; Beetz, M. Towards 3D Point cloud based object maps for household environments. *Robot. Auton. Syst.* **2008**, *56*, 927–941. [CrossRef]
45. Schinor, E.H.; Cristofani-Yaly, M.; Bastianel, M.; Machado, M.A. Sunki mandarin vs Poncirus trifoliata hybrids as rootstocks for Pera sweet orange. *J. Agric. Sci.* **2013**, *5*, 190. [CrossRef]
46. Yan, Z.; Liu, R.; Cheng, L.; Zhou, X.; Ruan, X.; Xiao, Y. A Concave Hull Methodology for Calculating the Crown Volume of Individual Trees Based on Vehicle-Borne LiDAR Data. *Remote Sens.* **2019**, *11*, 623. [CrossRef]
47. Lecigne, B.; Delagrange, S.; Messier, C. Exploring trees in three dimensions: VoxR, a novel voxel-based R package dedicated to analysing the complex arrangement of tree crowns. *Ann. Bot.* **2017**, *121*, 589–601. [CrossRef] [PubMed]
48. Cheng, G.; Wang, J.; Yang, J.; Zhao, Z.; Wang, L. Calculation Method of 3D Point Cloud Canopy Volume Based on Improved α-shape Algorithm. *Trans. Chin. Soc. Agric. Mach* **2021**, *52*, 175–183.
49. Zhou, H.-k.; Li, H.-w.; Zhao, X.; Guo, C.-l.; Li, B.-l. A Tree Crown Volume Calculation Method Based on Adaptive Slice of Point Cloud. *J. Northwest For. Univ.* **2023**, *38*, 189–195+202.
50. Edelsbrunner, H.; Kirkpatrick, D.; Seidel, R. On the shape of a set of points in the plane. *IEEE Trans. Inf. Theory* **1983**, *29*, 551–559. [CrossRef]
51. Fernández-Sarría, A.; Martínez, L.; Velázquez-Martí, B.; Sajdak, M.; Estornell, J.; Recio, J.A. Different methodologies for calculating crown volumes of Platanus hispanica trees using terrestrial laser scanner and a comparison with classical dendrometric measurements. *Comput. Electron. Agric.* **2013**, *90*, 176–185. [CrossRef]
52. Zhi, Y.; Zhang, Y.; Chen, H.; Yang, K.; Xia, H. A method of 3d point cloud volume calculation based on slice method. In Proceedings of the 2016 International Conference on Intelligent Control and Computer Application (ICCA 2016), Zhengzhou, China, 16–17 January 2016; pp. 155–158.
53. Jian, C.; Zheng, Y.; Liu, Y.; Ma, Y.; Yi, S.; Lü, Q.; Xie, R. Improving Detection of Mature Citrus Fruit Based on Target Detection Algorithm YOLOv5s. *South China Fruits* **2024**, *53*, 224–231.
54. Wang, D.; Ma, C.; Cao, J.; Wu, X.; Wu, Q.; Liu, L.; Chen, J.; Sun, J. Research and Application Progress of Digital Technology for Citrus Production. *South China Fruits* **2023**, *52*, 228–235.

Disclaimer/Publisher's Note: The statements, opinions and data contained in all publications are solely those of the individual author(s) and contributor(s) and not of MDPI and/or the editor(s). MDPI and/or the editor(s) disclaim responsibility for any injury to people or property resulting from any ideas, methods, instructions or products referred to in the content.